NATURAL FREQUENCIES OF ROTATING UNIFORM BEAMS WITH CORIOLIS EFFECTS

S. M. Hashemi* **and** **M. J. Richard**

Department of Mechanical Engineering, Laval University

Québec, Québec, Canada G1K 7P4

Tel. (418) 656-2190, Fax. (418) 656-7415, E-mail: mrichard@gmc.ulaval.ca

ABSTRACT

A Dynamic Finite Element (DFE) for vibrational analysis of rotating assemblages composed of beams is presented in which the complexity of the acceleration, due to the presence of gyroscopic, or Coriolis forces, is taken into consideration. The dynamic trigonometric shape functions of uncoupled bending and axial vibrations of an axially loaded uniform beam element are derived in an exact sense. Then, exploiting the Principle of Virtual Work together with the nodal approximations of variables, based on these dynamic shape functions, leads to a single frequency dependent stiffness matrix which is Hermitian and represents both mass and stiffness properties. A Wittrick-Williams algorithm, based on a Sturm sequence root counting technique, is then used as the solution method. The application of the theory is demonstrated by two illustrative examples of vertical and radial beams where the influence of Coriolis forces on natural frequencies of the clamped-free rotating beams is demonstrated by numerical results.

*Presently Assistant Professor in Aerospace Engineering, ryerson University, toronto, Ontario, CANADA

NOMENCLATURE

D_a denominator in the expressions of N_{1a} and N_{2a} (extensional shape functions),
D_{fz} denominator of N_{1fz},N_{2fz},N_{3fz} and N_{4fz}, (in-plane (lead-lag) flexural shape functions),
D_{fy} denominator of N_{1f},N_{2f},N_{3f} and N_{4f} (out-of-plane (flapping) flexural shape functions),
D_t denominator in the expressions of N_{1t} and N_{2t} (torsional shape functions),
H_a $= EA$ Extensional Rigidity,
H_{fz} $= EI_{zz}$ Flexural Rigidity,
H_{fy} $= EI_{yy}$ Flexural Rigidity,
H_t $= GJ$ Torsional Rigidity,
$[K_{DS}]$ overall dynamic stiffness matrix,
$[K_{DS}^{\Delta}]$ upper triangular matrix obtained from K_{DS},
$[K_{DS}]^k$ elementary DFE stiffness matrix,
$\mathcal{W}$ total virtual work,
$\mathcal{W}_{\mathcal{INT}}$ internal virtual work,
$\mathcal{W}_{\mathcal{EXT}}$ external virtual work,
$\mathcal{W}^k$ discretized elementary virtual work,
$\mathcal{W}_a^k$ the part of W^k corresponding to the extension,
$\mathcal{W}_{fz}^k$ the bending (in-plane) part of W^k,
$\mathcal{W}_{fy}^k$ the bending (out-of plane) part of W^k,
$\mathcal{W}_t^k$ the part of W^k corresponding to the torsion,
l_k the length of element "k",
m $= \rho A$; mass per unit length,
u extensional displacement,
U amplitude of the extensional displacement,
δU test function due to extensional displacement,
v lead-lag flexural displacement,
V amplitude of the lead-lag flexural displacement,
δV test function due to lead-lag flexural displacement,
w flapping flexural displacement,
W amplitude of the flapping flexural displacement,
δW test function due to flapping flexural displacement,
ψ torsional rotation,
Ψ amplitude of the torsional rotation,
$\delta\Psi$ test function due to torsional displacement,
ξ $= \frac{s}{l_k}$; elementary local coordinate; $0 \leq \xi \leq 1$,
Ω rotating speed,
ω rotary frequency.

INTRODUCTION

There has in recent years been an upsurge of interest in the vibrational analysis of elastic rotating structures. Numerous structural configurations such as helicopter, turbine and compressor blades, spinning spacecraft, satellites, and also rotating shafts and linkages, fall into this category. The essential feature that distinguishes such systems from non-rotating ones is, in general, the complexity of the accelerations which act throughout the system. In addition to the accelerations resulting from elastic structural deformations, the equations of motion may involve significant gyroscopic, Coriolis, and centripetal accelerations. Also, the stiffness characteristics of the structure may be modified by the steady state internal loads induced by the centrifugal forces. The "classic" stiffening effect experienced by a rotating beam is discussed in many texts [1-7] and most of the work reported on spinning structures [2-4]

has been concerned with *discrete* models in which the deformation of the system from its state of steady rotation is described by a time-dependent displacement vector, containing a finite number of N components. The finite element method, lumped mass, and Rayleigh-Ritz method provide examples of such methods. In finite element formulations, because of their completeness and ease of manipulation, polynomials are often used. In this case, approximate member equations in the form of mass and static stiffness matrices, are used. The Dynamic Stiffness Matrix (DSM) method has certain advantages over the conventional finite element method, particularly when higher frequencies and better accuracies of results are required. This is true because the properties obtained from the method of DSM are based on the closed form analytical solution of the differential equation of the element and hence are justifiably called "exact". However, the application of the DSM method is limited to special cases. When the axial and transversal (in-plane and out-of-plane) vibrations of beams rotating at constant angular velocity has to be studied, the effect of the steady state tension (centrifugal force) is not negligible. In addition, the centrifugal force can not be assumed to be constant along the length of the member. Hence, as it will be discussed later, the governing differential equations of motion, in this case, contain the variable coefficients which makes it impossible to solve them analytically. The only way of deriving the exact DSM of the member, in that case, is by numerical integration of the governing equations of motion [8].

The Dynamic Finite Element (DFE) approach developed here produces accurate solutions for vibration of spinning assemblages composed of beam elements, in the presence of the Coriolis forces.

This method can be considered as a combination of the well-known weighted residual method, as used in the conventional FEM, and some interesting features of the DSM approach. The effect of the variable centrifugal force is also taken into account by an approach presented before [9]. The exact solution of the equations governing the uncoupled bending and extensional vibrations of an axially loaded beam are first obtained. The employment of these solutions as basis functions then leads to the frequency dependent (dynamic) trigonometric shape functions. The Principle of Virtual Work (PVW) together with the nodal approximations of variables, based on the dynamic shape functions, are then utilized to derive the elementary (dynamic) stiffness matrix. The stiffness matrix represents both mass and stiffness properties and, in this case, is Hermitian. Then, the elementary stiffness matrices are assembled directly, to make the global complex Hermitian stiffness matrix. The theorem presented by Wittrick andWilliams [8], based on Sturm sequence properties of Dynamic Stiffness Matrix of structures, can then be used for the systematic calculation of the natural frequencies of the system. The same theorem is also applicable for either a discrete system which is assembled from sub-structures, or an assembly of distributed mass members and is identical to a corresponding one for non-spinning structures [10-13] Numerical checks are performed to confirm the predictability and the accuracy of the theory. The effect of the centrifugal, centripetal and the gyroscopic, or Coriolis forces on the eigenfrequencies of beams is demonstrated for two examples by comparing the different cases as non-rotating beam, rotating beam neglecting the gyroscopic forces and rotating beam when the Coriolis forces are taken into consideration. The advantage of this approach, when compared to the exact DSM method, is that it can be extended to more complex cases such as rotating beams with variable geometry and mechanical properties.

The DFE approach has been applied, in different occasions, to the vibrational analysis of non-uniform beams [14], the rotating uniform and tapered beams [7, 9, 15] and coupled flexural-torsional beam vibrations [16, 17] for which, the Dynamic Stiffness Matrices were real.

MATHEMATICAL MODEL

The Governing Equations of Motion

Here, the application of the DFE method to the natural frequency calculation of a rotating beam-made frame is discussed. Consider a rigidly jointed two-dimensional frame attached to a rigid hub which is spinning with constant velocity Ω about an axis in the plane of the frame. The members of the frame are supposed to be uniform and to have distributed mass. A simple example of such a frame is shown in Figure (1). For simplicity it is also assumed that the shear centre and the centrid of the cross section of each member coincide (i.e., no bending-torsion coupling), and that the principal axes of the cross section lie within and prependicular to the plane of the frame.

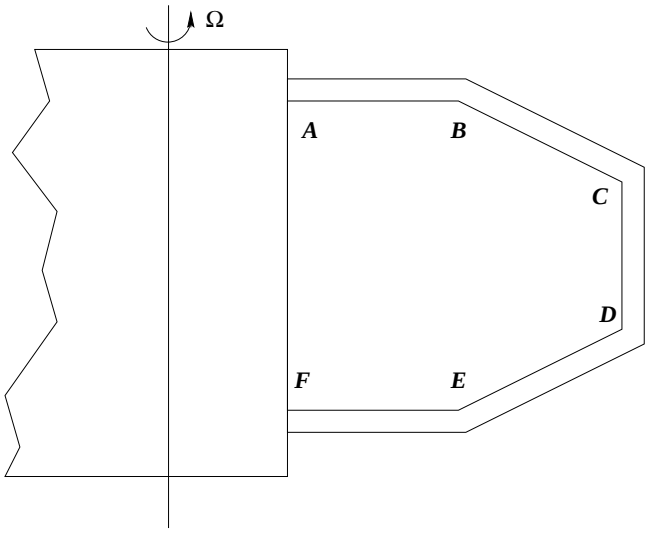

FIGURE 1: AN EXAMPLE OF A SPINNING TWO-DIMENSIONAL FRAME.

Consider then a single, straight, uniform, Euler-Bernoulli beam, representing a typical member of the frame, as shown in Figure (2). Introducing a set of cartesian coordinate system (x,y,z), in the *undeformed* state the member lies in x-z plane, inclined at an constant angle α to the x direction. We assume here that Ω is well below the critical speed at which an instability of the structure, in the form of a divergence may occur [8]. Including the rotating inertia at the base (i.e., the rigid hub) and a payload at the tip of a rotating beam has been addressed by Bellezza *et al.* [18], but in this study these effects are not taken into account and we only consider small vibrations about the steady *deformed* state. In this case, the governing differential equations of motion for an element is (see Appendix A):

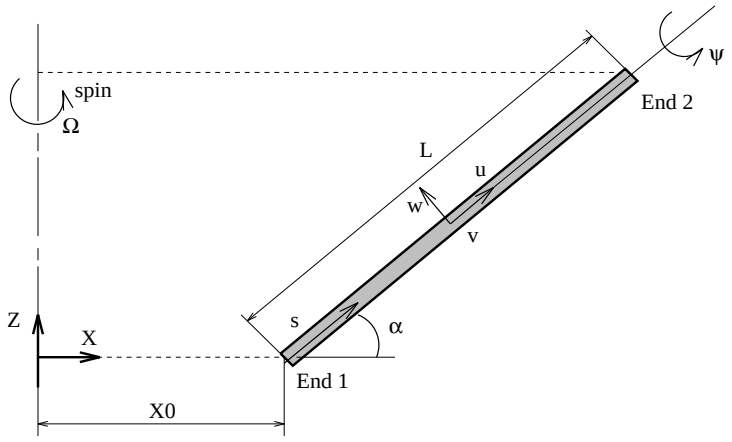

FIGURE 2: AN INDIVIDUAL MEMBER OF A FRAME.

$$\{-(EA)\frac{\partial^2 u}{\partial s^2} - m\ u\ \Omega^2\ \cos^2\alpha + m\ \frac{\partial^2 u}{\partial t^2}\}\ +$$

$$m\ w\ \Omega^2\ \cos\alpha\ \sin\alpha - 2\ m\ \frac{\partial v}{\partial t}\ \Omega\ \cos\alpha = 0 \tag{1}$$

$$\{(H_{fz})\frac{\partial^4 v}{\partial s^4} - \frac{\partial}{\partial s}(T\frac{\partial v}{\partial s}) - m\ v\Omega^2 + m\ \frac{\partial^2 v}{\partial t^2}\}\ +$$

$$2\ m\ \frac{\partial u}{\partial t}\ \Omega\ \cos\alpha - 2\ m\ \frac{\partial w}{\partial t}\ \Omega\ \sin\alpha = 0 \tag{2}$$

$$\{(H_{fy})\frac{\partial^4 w}{\partial s^4} - \frac{\partial}{\partial s}(T\frac{\partial w}{\partial s}) - m\ w\Omega^2\sin^2\alpha + m\ \frac{\partial^2 w}{\partial t^2}\}\ +$$

$$2\ m\ \frac{\partial v}{\partial t}\ \Omega\ \sin\alpha + m\ u\ \Omega^2\ \cos\alpha\ \sin\alpha = 0 \tag{3}$$

$$\left\{\frac{(H_t)}{m\mathcal{R}^2}\frac{\partial^2\psi}{\partial s^2} - \frac{\partial^2\psi}{\partial t^2}\right\} = 0 \tag{4}$$

In these equations m is the mass per unit length, EA the extensional rigidity, H_t the torsional rigidity, H_{fz} and H_{fy} the flexural rigidities for bending in v and w directions, respectively, $\mathcal{R}$ the polar radius of gyration of the cross section, and T is the steady state tension in the member. Also, u, v, and w denote the displacements from the *deformed* steady state.

If the displacements are varying harmonically with time, at a frequency ω, one can write

$$\{u, v, w, \psi\} = \{U(s), V(s), W(s), \Psi(s)\}e^{i\omega t} \tag{5}$$

and obtain the following set of ordinary differential equations:

$$\{-(\frac{EA}{m})\frac{d^2U}{ds^2} - (\Omega^2\cos^2\alpha + \omega^2)U\} \; - \; (2i\omega\Omega\cos\alpha)V \; + \; (\Omega^2\cos\alpha.\sin\alpha)W = 0. \tag{6}$$

$$(2i\omega\Omega\cos\alpha)U \; + \; \{(\frac{H_{fz}}{m})\frac{d^4V}{ds^4} - (\frac{1}{m})\frac{d}{ds}(T\frac{dV}{ds}) - (\Omega^2+\omega^2)V\} \; - \; (2i\omega\Omega\sin\alpha)W = 0. \tag{7}$$

$$(\Omega^2\cos\alpha.\sin\alpha)U \; + (2i\omega\Omega\sin\alpha)V \; + \; \{(\frac{H_{fy}}{m})\frac{d^4W}{ds^4} - (\frac{1}{m})\frac{d}{ds}(T\frac{dW}{ds}) - (\Omega^2\sin^2\alpha + \omega^2)W\} = 0. \tag{8}$$

$$(\frac{H_t}{m\mathcal{R}^2})\frac{d^2\Psi}{ds^2} + \omega^2\Psi = 0. \tag{9}$$

Equation (9) governs the torsional vibration, which is uncoupled from the longitudinal (U) and two bending (V and W) vibrations. Moreover it does not involve the velocity of spin, Ω, and the dynamic torsional stiffness coefficients are the same as for a non-spinning beam.

Unfortunately it is not such a simple matter to solve equations (6 -8) for the longitudinal and bending vibrations. Not only are these equations coupled, but the steady state tension T will in general be a function of s, because if α is different than 90^o there will be a component of the steady state radial acceleration, $x_0\Omega^2$, along the member. This means that the terms involving T in equations (7) and (8), which arise from the effect of the tension on the bending moments, will introduce variable coefficients into the differential equations and make it impossible to obtain an analytical solution. The only way of deriving the "exact" Dynamic Stiffness Matrix of the member in that case is by numerical integration of equations (6-8) by using for example the Runge-Kutta method [8]. Another more expedient way of dealing with a member with varying T, as proposed by Wittrick and Williams [8] would be to break it down into several members, joined end to end, of such length that they can all reasonably be assumed to have constant T. Under these circumstances it is possible to write down a general solution for U, V and W, involving 10 arbitrary constants

of integration. The calculation of the tenth order dynamic stiffness matrix will of course involve complex arithmetics and the application of the method will be limited to special cases (i.e., the governing differential equations with constant coefficients).

Integral Formulation

The use of the Bubnov-Galerkin weigted residual method leads to the integral form associated to equations (6) – (8). Then, applying an appropriate number of integrations by parts allows us to diminish the derivatives order and the weak integral form is then obtained as:

$$\begin{aligned}\mathcal{W}_a = & \int_0^L \left\{(EA)\delta U^{'}U^{'} - m\ (\Omega^2\cos^2\alpha + \omega^2)\delta U U\right\} ds\ - \\ & \left[(EA)\delta U\ U^{'}\right]_0^L\ - \int_0^L \delta U(2\ m\ i\omega\Omega\cos\alpha)V ds\ + \\ & \int_0^L \delta U(m\ \Omega^2\cos\alpha.\sin\alpha)W ds \end{aligned} \tag{10}$$

$$\begin{aligned}\mathcal{W}_{fz} = & \int_0^L \delta V\ (2\ m\ i\ \omega\ \Omega\ \cos\alpha)\ U\ ds\ + \\ & \int_0^L \left\{(H_{fz})\delta V^{''}V^{''} - \delta V^{'}(T)V^{'} - m\ (\Omega^2+\omega^2)\delta V V\right\} ds\ + \\ & \left[H_{fz}(\delta V V^{'''} - \delta V^{'}V^{''}) - (T)\delta V V^{'}\right]_0^L\ - \\ & \int_0^L \delta V(2\ m\ i\omega\Omega\sin\alpha)W ds \end{aligned} \tag{11}$$

$$\begin{aligned}\mathcal{W}_{fy} = & \int_0^L \delta W\ (m\ \Omega^2\ \cos\alpha.\sin\alpha)\ U\ ds\ + \\ & \int_0^L \delta W(2\ mi\omega\Omega\sin\alpha)V ds\ + \int_0^L \left\{(H_{fy})\delta W^{''}W^{''}\ - \right. \\ & \left.\delta W^{'}(T)W^{'}\ - m\ (\Omega^2\sin^2\alpha + \omega^2)\delta W W\right\} ds\ + \\ & \left[H_{fy}(\delta W W^{'''} - \delta W^{'}W^{''}) - (T)\delta W W^{'}\right]_0^L \end{aligned} \tag{12}$$

Here, U, V and W are solution functions and $\delta U, \delta V$ and δW are test functions. Both quantities are defined in the same approximation space. The test functions must satisfy the following boundary condition:

$$\text{test functions} = 0, \text{ on } S_u$$

where S_u represents the part of boundary (S) where solution functions $(U, V$ and $W)$ are specified.

For Clamped boundary condition, for example, $\delta U = \delta V = \delta V^{'} = \delta W = \delta W^{'} = 0$, and force terms are zero at a free end. Expressions (10) – (12) also satisfy the Principle of Virtual Work (PVW)

$$\mathcal{W} \;=\; \mathcal{W}_{INT} - \mathcal{W}_{EXT} = 0$$

where

$$\mathcal{W}_{INT} \;=\; \mathcal{W}_a + \mathcal{W}_{fz} + \mathcal{W}_{fy} \tag{13}$$

and $\mathcal{W}_{EXT} = 0$, for free vibrations.

If the domain is discretized by a number of 2-node elements [19, 20], we have (see Figure 3):

$$\mathcal{W} = \mathcal{W}_{INT} = \sum_{k=1}^{NE} \mathcal{W}^k = 0 \tag{14}$$

where

$$\mathcal{W}^k = \mathcal{W}^k{}_a + \mathcal{W}^k{}_{fz} + \mathcal{W}^k{}_{fy} \tag{15}$$

and

$$\begin{aligned}\mathcal{W}^k{}_a = \int_{x_j}^{x_{j+1}} \Big\{(EA)\delta U^{'}\; U^{'} - m(\Omega^2\cos^2\alpha + \omega^2)\delta U U\Big\}\, ds \\ - \int_{x_j}^{x_{j+1}} \delta U\; (2\; m\; i\omega\; \Omega\;\; \cos\alpha)\; V\; ds \\ + \int_{x_j}^{x_{j+1}} \delta U\; (m\; \Omega^2\;\; \cos\alpha\; .\; \sin\alpha)\; W\; ds\end{aligned} \tag{16}$$

$$\begin{aligned}\mathcal{W}^k{}_{fz} \;=\; \int_{x_j}^{x_{j+1}} \delta V\; (2\; m\; i\; \omega\Omega\;\; \cos\alpha)\; U\; ds \;+ \\ \int_{x_j}^{x_{j+1}} \Big\{\delta V^{''}(H_{fz})V^{''} + \delta V^{'}(T)V^{'} - m(\Omega^2 + \omega^2)\delta V V\Big\}\, ds \\ - \int_{x_j}^{x_{j+1}} \delta V(2\; m\; i\omega\Omega\sin\alpha)W ds\end{aligned} \tag{17}$$

$$\begin{aligned}\mathcal{W}_{fy} = \int_{x_j}^{x_{j+1}} \delta W(m\;\Omega^2\;\; \cos\alpha.\sin\alpha)\; U\; ds \;+ \\ \int_{x_j}^{x_{j+1}} \delta W(2\; mi\omega\Omega\sin\alpha)V ds \;+ \int_{x_j}^{x_{j+1}} \Big\{\delta W^{''}(H_{fy})W^{''} \;+ \\ \delta W^{'}(T)W^{'} - m\;(\Omega^2\sin^2\alpha + \omega^2)\delta W\; W\Big\}\, ds\end{aligned} \tag{18}$$

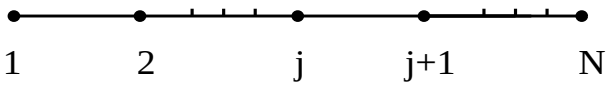

FIGURE 3: The domain, discretized by a number of 2-node elements.

Each element is defined by nodes $j, j+1$ with corresponding coordinates.

After an appropriate number of integration by parts on the elementary equations, the relation $\mathcal{W}^k$ may also be written in the following form

$$\mathcal{W}^k{}_a = \int_{x_j}^{x_{j+1}} -U\left\{(EA)\delta U'' + m(\Omega^2\cos^2\alpha + \omega^2)\delta U\right\} ds +$$

$$\left[(EA)\ \delta U'\ U\right]_{x_j}^{x_{j+1}} - \int_{x_j}^{x_{j+1}}\ \delta U\ (2\ m\ i\ \omega\ \Omega\ \cos\alpha)\ V\ ds\ -$$

$$\int_{x_j}^{x_{j+1}} \delta U\ (m\ \Omega^2\ \cos\alpha.\sin\alpha)W ds \tag{19}$$

$$\mathcal{W}^k{}_{fz} = \int_{x_j}^{x_{j+1}}\ \delta V\ (2\ m\ i\ \omega\ \Omega\ \cos\alpha)\ U\ ds\ +$$

$$\int_{x_j}^{x_{j+1}} V\left\{(H_{fz})\ \delta V'''' - (T)\ \delta V'' - m\ (\Omega^2+\omega^2)\delta V\right\} ds\ +$$

$$\left[(H_{fz})\left\{\delta V''V'\ -\ \delta V'''V\right\} + (T)\ \delta V'V\right]_{x_j}^{x_{j+1}}\ -$$

$$\int_{x_j}^{x_{j+1}} \delta V(2\ m\ i\omega\Omega\sin\alpha)W ds \tag{20}$$

$$\mathcal{W}_{fy} = \int_{x_j}^{x_{j+1}} \delta W\ (m\ \Omega^2\ \cos\alpha.\sin\alpha)\ U\ ds\ +$$

$$\int_{x_j}^{x_{j+1}} \delta W(2\ mi\omega\Omega\sin\alpha)V ds\ + \int_{x_j}^{x_{j+1}} W\left\{(H_{fz})\delta V'''' -\right.$$

$$\left.(T)\ \delta V''\ -\ m\ (\Omega^2\ \sin^2\alpha\ +\ \omega^2)\ \delta W\ \right\}\ ds\ +$$

$$\left[(H_{fy})\left\{\delta W''W'\ -\ \delta W'''W\right\} + (T)\ \delta W'W\right]_{x_j}^{x_{j+1}} \tag{21}$$

The admissibility condition for finite element approximation is controlled by equations (10 -12). The approximation for $V,\ \delta V,\ W$ and δW is of C^1-type, assuring continuity of $V,\ V_{,x},\ W$ and $W_{,x}$ at each node, and the approximation for $\Psi,\ \delta\Psi$ is of C^0-type. Equations (19 -21) present simply a way of evaluating equations (16 -18) at the element level.

Dynamic Finite Element (DFE) Method

When coefficients H_{fz}, H_{fy}, H_t, $T(x)$, $m(x)$, etc. are not constant, it becomes difficult and cumbersome to obtain the exact model. In this study, we propose an intermediate approach, where the interpolation functions are obtained, with averaged value parameters over each element, which are the solutions of the uncoupled form of the governing differential equations of motion. The method is briefly explained here for the case of a "uniform rotating beam", but it can be extended to more complex cases as nonuniform beams [9, 14, 15].

The influence of variable parameters (here $T(x)$), can be taken into account by rewriting the equations (15-18) as:

$$\mathcal{W}^k = \mathcal{W}^k{}_a + \mathcal{W}^k{}_{fz} + \mathcal{W}^k{}_{fy} \tag{22}$$

where

$$\begin{aligned}\mathcal{W}^k{}_a = \int_{x_j}^{x_{j+1}} \left\{\delta U^{'}(EA)U^{'} - m(\Omega^2\cos^2\alpha + \omega^2)\delta U U\right\} ds - \\ \int_{x_j}^{x_{j+1}} \delta U(2\ m\ i\omega\Omega\cos\alpha)V\, ds \\ + \int_{x_j}^{x_{j+1}} \delta U(m\ \Omega^2\cos\alpha.\sin\alpha)W\, ds\end{aligned} \tag{23}$$

$$\begin{aligned}\mathcal{W}^k{}_{fz} = \int_{x_j}^{x_{j+1}} \delta V(2\ m\ i\ \omega\ \Omega\ \cos\alpha)\ U\ ds\ + \\ \int_{x_j}^{x_{j+1}} \left\{\delta V^{''}(H_{fz})V^{''} + \delta V^{'}(\bar{T})V^{'} - m(\Omega^2+\omega^2)\delta V V\right\} ds - \\ \int_{x_j}^{x_{j+1}} \delta V^{'}(T_{DEV})V^{'} ds - \int_{x_j}^{x_{j+1}} \delta V(2\ m\ i\omega\Omega\sin\alpha)W\, ds\end{aligned} \tag{24}$$

$$\begin{aligned}\mathcal{W}_{fy} = \int_{x_j}^{x_{j+1}} \delta W(m\ \Omega^2\ \cos\alpha.\sin\alpha)\ U\ ds\ + \\ \int_{x_j}^{x_{j+1}} \delta W(2\ m\ i\ \omega\ \Omega\ \sin\alpha)\ V\ ds\ + \int_{x_j}^{x_{j+1}} \left\{\delta W^{''}(H_{fy})W^{''} + \right. \\ \left. \delta W^{'}(\bar{T})W^{'} - m\ (\Omega^2\sin^2\alpha + \omega^2)\delta W\ W\right\} ds\ - \\ \int_{x_j}^{x_{j+1}} \delta W^{'}(T_{DEV})W^{'} ds\end{aligned} \tag{25}$$

and

$$T_{DEV} = (\bar{T} - T(x)); \quad \bar{T} = \int_{xj}^{x_{j+1}} T(s)ds/(x_{j+1} - xj).$$

The relation $\mathcal{W}^k$ may also be written as:

$$\mathcal{W}^k{}_a = \int_0^1 -U \underbrace{[(\frac{EA}{l_k})\delta U'' + ml_k(\Omega^2 \cos^2\alpha + \omega^2)\delta U]}_{*} d\xi +$$

$$\left[(\frac{EA}{l_k})\delta U' \; U\right]_0^1 - \int_0^1 \delta U(2\; ml_k\; i\omega\Omega\cos\alpha)V d\xi -$$

$$\int_0^1 \delta U(ml_k\; \Omega^2 \cos\alpha.\sin\alpha)W d\xi \tag{26}$$

$$\mathcal{W}^k{}_{fz} = \int_0^1 \delta V(2\; ml_k\; i\omega\Omega\cos\alpha)U d\xi \; +$$

$$\int_0^1 V \underbrace{\left((\frac{H_{fz}}{l_k^3})\; \delta V'''' - (\frac{\bar{T}}{l_k})\; \delta V'' - ml_k\; (\Omega^2 + \omega^2)\delta V\right)}_{**} d\xi +$$

$$\left[(\frac{H_{fz}}{l_k^3})\left\{\delta V'' V' \; - \; \delta V''' V\right\} + (\frac{\bar{T}}{l_k})\; \delta V' V\right]_0^1 -$$

$$(\frac{1}{l_k})\int_0^1 \delta V'(T_{DEV})V' d\xi \; - \int_0^{l_k} \delta V(2\; ml_k\; i\omega\Omega\sin\alpha)W d\xi \tag{27}$$

$$\mathcal{W}_{fy} = \int_0^{l_k} \delta W(ml_k\; \Omega^2\cos\alpha.\sin\alpha)U d\xi \; +$$

$$\int_0^1 W \underbrace{\left((\frac{H_{fz}}{l_k^3})\delta V'''' - (\frac{\bar{T}}{l_k})\delta V'' - ml_k(\Omega^2\sin^2\alpha + \omega^2)\delta W\right)}_{***} d\xi -$$

$$\int_0^1 \delta W(2\; ml_k i\omega\Omega\sin\alpha)V d\xi \; + (\frac{1}{l_k})\int_0^1 \delta W'(T_{DEV})W' d\xi \; +$$

$$\left[(\frac{H_{fy}}{l_k^3})\left\{\delta W'' W' \; - \; \delta W''' W\right\} \; + \; (\frac{\bar{T}}{l_k})\; \delta W' W\right]_0^1 \tag{28}$$

where $\xi = \frac{s}{l_k}$, and s and l_k represent the k^{th} element's local coordinate and its length, respectively $(0 \leq s \leq l_k)$. The equations (26-28) are simply a different way of evaluating equations (15-18) at the element level.

Then, to obtain the Dynamic Finite Element model δU, U, δV, V,δW and W, are approximated so that (*), (**) and (***) vanish:

$$\delta U =< P(\xi) >_a *\{\delta a\} \quad ; \quad U =< P(\xi) >_a *\{a\} \tag{29}$$

$$\delta V =< P(\xi) >_{fz} *\{\delta b\} \quad ; \quad V =< P(\xi) >_{fz} *\{b\} \tag{30}$$

$$\delta W =< P(\xi) >_{fy} *\{\delta c\} \quad ; \quad W =< P(\xi) >_{fy} *\{c\} \tag{31}$$

One can note that the torsion (Eq. (9)) can be easily introduced in the development to include the torsional degrees of freedom (DOF) in the element. In this case, the torsion is also considered to be included. Hence we can write

$$\delta \Psi =< P(\xi) >_t *\{\delta d\} \quad ; \quad \Psi =< P(\xi) >_t *\{d\} \tag{32}$$

where$< P(\xi) >_a$, $< P(\xi) >_{fz}$, $< P(\xi) >_{fy}$ and $< P(\xi) >_t$ are found to be

$$< P(\xi) >_a \;=\; < \cos(\eta\xi) \; ; \; \frac{\sin(\eta\xi)}{\eta} > \tag{33}$$

$$\begin{aligned} < P(\xi) >_{fz} \;=\; & < \cos(\alpha_z\xi) \; ; \; \frac{\sin(\alpha_z\xi)}{\alpha_z} \; ; \\ & \frac{\cosh(\beta_z\xi) - \cos(\alpha_z\xi)}{{\alpha_z}^2 \; + \; {\beta_z}^2} \; ; \frac{\sinh(\beta_z\xi) - \sin(\alpha_z\xi)}{{\alpha_z}^3 \; + \; {\beta_z}^3} > \end{aligned} \tag{34}$$

$$\begin{aligned} < P(\xi) >_{fy} \;=\; & < \cos(\alpha_y\xi) \; ; \; \frac{\sin(\alpha_y\xi)}{\alpha_y} \; ; \\ & \frac{\cosh(\beta_y\xi) - \cos(\alpha_y\xi)}{{\alpha_y}^2 \; + \; {\beta_y}^2} \; ; \frac{\sinh(\beta_y\xi) - \sin(\alpha_y\xi)}{{\alpha_y}^3 \; + \; {\beta_y}^3} > \end{aligned} \tag{35}$$

$$< P(\xi) >_t \;=\; < \cos(\tau\xi) \; ; \; \frac{\sin(\tau\xi)}{\tau} > \tag{36}$$

where;

$$\alpha_z \; , \; \beta_z \;=\; \frac{1}{[2 * A_z]^{\frac{1}{2}}}\{ \; -B_z \; \pm \; |B_z^2 - 4A_z * C_z|^{\frac{1}{2}} \; \}^{\frac{1}{2}};$$

$$\alpha_y \; , \; \beta_y \;=\; \frac{1}{[2 * A_y]^{\frac{1}{2}}}\{ \; -B_y \; \pm \; |B_y^2 - 4A_y * C_y|^{\frac{1}{2}} \; \}^{\frac{1}{2}};$$

$$\eta \;=\; l_k\sqrt{\frac{m\;(\Omega^2\;\cos^2\alpha\;+\;\omega^2)}{H_a}}; \tau \;= \omega l_k \mathcal{R}(m/Ht)^{1/2}. \tag{37}$$

and;

$$A_z = \frac{H_{fz}}{l_k^3}\quad, B_z = -(\frac{\bar{T}}{l_k})\quad, C_z = -ml_k(\Omega^2+\omega^2),$$

$$A_y = \frac{H_{fy}}{l_k^3}\quad, B_y = -(\frac{\bar{T}}{l_k})\quad, C_y = -ml_k(\Omega^2\sin^2\alpha+\omega^2).$$

Considering $< a >$, $< b >$, $< c >$ and $< d >$ as nodal variables $< U_1; U_2 >$, $< V_1; V_1^{'}; V_2; V_2^{'} >$, $< W_1; W_1^{'}; W_2; W_2^{'} >$, $< \Psi_1; \Psi_2 >$, respectively, we obtain

$$\{U_n\} = [P_n]_a * \{a\} \tag{38}$$

$$\{V_n\} = [P_n]_{fz} * \{b\} \tag{39}$$

$$\{W_n\} = [P_n]_{fy} * \{c\} \tag{40}$$

$$\{\Psi_n\} = [P_n]_t * \{d\} \tag{41}$$

and hence, the approximation (29)-(32) in nodal variables is written as:

$$U(\xi) \;=\; < P(\xi) >_a [P_n]_a^{-1}\{U_n\} \;=\; < N(\xi) >_a \{U_n\} \tag{42}$$

$$V(\xi) \;=\; < P(\xi) >_{fz} [P_n]_{fz}^{-1}\{V_n\} \;=\; < N(\xi) >_{fz} \{V_n\} \tag{43}$$

$$W(\xi) \;=\; < P(\xi) >_{fy} [P_n]_{fy}^{-1}\{W_n\} = \;< N(\xi) >_{fy} \{W_n\} \tag{44}$$

$$\Psi(\xi) \;=\; < P(\xi) >_t [P_n]_t^{-1}\{\Psi_n\} \;=\; < N(\xi) >_t \{\Psi_n\} \tag{45}$$

and can be rearranged as:

$$\left\{\begin{array}{c} U(\xi) \\ V(\xi) \\ W(\xi) \\ \Psi(\xi) \end{array}\right\} \;=\; [N] * \{w_n\} \tag{46}$$

where,

$$\{w_n\} \;=\; < U_1\; V_1\; V_1^{'}\; W_1\; W_1^{'}\; \Psi_1\; U_2\; V_2\; V_2^{'}\; W_2\; W_2^{'}\; \Psi_2 >^T; \tag{47}$$

and

$$[\ N\ ] = \begin{bmatrix} < N_{\ a} > \\ < N_{\ fz} > \\ < N_{\ fy} > \\ < N_{\ t} > \end{bmatrix} = \begin{bmatrix} N_1(\omega)_a & 0 & 0 & 0 & 0 & 0 \\ 0 & N_1(\omega)_{fz} & N_2(\omega)_{fz} & 0 & 0 & 0 \\ 0 & 0 & 0 & N_1(\omega)_{fy} & N_2(\omega)_{fy} & 0 \\ 0 & 0 & 0 & 0 & 0 & N_1(\omega)_t \end{bmatrix}$$

$$\begin{bmatrix} N_2(\omega)_a & 0 & 0 & 0 & 0 & 0 \\ 0 & N_3(\omega)_{fz} & N_4(\omega)_{fz} & 0 & 0 & 0 \\ 0 & 0 & 0 & N_3(\omega)_{fy} & N_4(\omega)_{fy} & 0 \\ 0 & 0 & 0 & 0 & 0 & N_2(\omega)_t \end{bmatrix} \tag{48}$$

are the frequency dependent dynamic shape functions, mentioned earlier. Their analytical expressions and graphical illustrations, together with the plot of the static and dynamic basis functions (i.e., $P_i(\omega)_{fz,i=1,2,3,4}$), for a uniform beam rotating in the hoerizontal plane, are given in Appendix B (see Figures 8,9 and 10). Similar approximations are also written for U, V, W and Ψ. Using equation (16-18) the DFE stiffness matrix is then obtained as:

$$\mathcal{W}^k =< \delta w_n > [K_{DS}]^k \{w_n\}; \tag{49}$$

where

$$[K_{DS}]^k = [K_{DS}]^k_{AV} + [K_{DS}]^k_{DEV} + [K_{DS}]^k_{COR} + [K_{DS}]^k_{CENT};$$

and

$[K_{DS}]^k =$ DFE stiffness matrix of the element k,
$[K_{DS}]^k_{AV} =$ $[K_{DS}]^k$, from constant axial force/element,
$[K_{DS}]^k_{DEV} = [K_{DS}]^k$, due to T variation,
$[K_{DS}]^k_{COR} =$ Hermitian Coriolis (gyroscopic) matrix,
$[K_{DS}]^k_{CENT} =$ Centrifugal stiffness matrix.

These matrices are given in detail in Appendix C.

It can be readily verified from equations (26-28 and 49) that if the Coriolis forces are neglected, the resultant stiffness matrix, reduces to the stiffness matrix representing the uncoupled flexural and

axial vibrations of a spinning uniform Euler-Bernoulli beam element [7]. Furthermore, if a rotating speed Ω is assumed to be equal to zero, the degenerated stiffness matrix of equation (14) becomes the stiffness matrix representing the uncoupled flexural and axial vibrations of a Euler-Bernoulli beam element [8, 11].

It can be also verified that when $\omega \rightarrow 0$, the functions of equations (34) and (35) become; $1; x; x^2; x^3$. Also, the functions of equations (33) and (36), in this case, change to $1; x$. The former, represent the expansion terms in the formulation of the "Hermite" beam element, in conventional finite element method, when flexural degrees of freedom are considered. The latter, correspond to the expansion terms, in a linear element formulation in conventional FEM, when the torsion (or axial displacement) of a beam element is studied. In this case, the dynamic shape functions presented in this paper become the corresponding shape functions actually used in static conventional FEM. Therefore, the dynamic stiffness matrix of equation (49) changes to the static stiffness matrix of a "Hermite" type beam element, wherein the torsion is included by using a linear approximation [19, 20]. The convergence of the DFE formulation, applied to the bending vibration of rotating beams, has been demonstrated and discussed in another paper published by the authors (see [15]).

APPLICATION OF THE THEORY

The expressions for the DFE stiffness matrix, $[K_{DS}]^k$, derived in the previous section, can be directly used to compute the natural frequencies and mode shapes of spinning blade-like structures (such as helicopter, propeller or turbine blades), plane or space rotating frames, or grillages consisting of beams in which the elastic axis and the inertial axis are coincident.

Elementary matrices then will have to be assembled in the usual way to form the overall dynamic stiffness matrix $[K_{DS}]$ of the final structure. The eigenvalue problem, for free vibrations, is found then to be as:

$$[K_{DS}] * \{W_n\} = \{0\} \tag{50}$$

where $[K_{DS}]$ is Hermitian. The natural frequencies are calculated from the equation (50) and the well-known Wittrick-Williams algorithm based on the Sturm sequence property of $[K_{DS}]$ (e.g. see [8]).

Suppose that ω denotes the circular frequency of the beam. Then it is known that j, the number of eigenvalues passed as ω is increased from zero to ω^*, is given by

$$j \;=\; j_0 \;+\; s\{K_{DS}\} \tag{51}$$

where $[K_{DS}]$ is the overall DSM (which is ω dependent) of the structure, evaluated at $\omega = \omega^*$; the *sign count* of $[K_{DS}]$, $s\{K_{DS}\}$, in this case, is defined as the number of reversals of sign between consecutive members of the sequence $H_0H_1H_2...H_m$, where $H_0 = +1$ and $H_r(\omega^*)$ is the leading principal minor of order r of the complete dynamic stiffness matrix $[K_{DS}(\omega^*)]$: i.e., the determinant of the matrix of the elements in the first r rows and columns of $[K_{DS}(\omega^*)]$. The sign count is easily computed by transforming $[K_{DS}]$ into upper triangular form K_{DS}^{Δ} by the usual form of Gauss elimination, in which rows are taken as pivotal in order and appropriate multiples of the pivotal row are added to (unscaled) succeeding rows to make all elements below the pivot zero. Note that the diagonal elements of K_{DS}^{Δ} are real, and it follows that $s\{K_{DS}\}$ is simply equal to the number of negative diagonal elements in K_{DS}^{Δ} [8]. j_0 (i.e., the number of natural frequencies of the beam still lying between $\omega = 0$ and $\omega = \omega^*$ when the displacement components to which K_{DS} corresponds are all zero), is equal to the sum of j_m while the summation extends over all elements. Within the limits of the theory developed in this paper, the constrained frequencies of an individual element, j_m, occur when one or more of the components of the matrices of equations (49) become infinite . This will occur when $D_a = 0$, $D_{fz} = 0$, $D_{fy} = 0$ or $D_t = 0$, which are respectively the denominators in axial, flexural and torsional dynamic shape functions, given in Appendix B. They lead, respectively, to the j_a, j_{fz}, j_{fy} and j_t values which can be evaluated from the existing procedures explained in different occasions [7, 9, 14, 15, 21, 22].

$D_a = sin(\eta) = 0$ and $D_t = sin(\tau) = 0$ are satisfied when $\eta = i\pi$ and $\tau = i\pi$, respectively, and hence

$$j_a \quad \text{is the highest integer} \leq \tfrac{\eta}{\pi},$$

and

$$j_t \quad \text{is the highest integer} \leq \tfrac{\tau}{\pi}.$$

Clearly is not so simple to find the j components arising from $D_{fz} = 0$ and $D_{fy} = 0$. However they can be obtained as follows [15, 21].

Consider the in-plane bending vibration of a simply supported axially loaded beam, treated as a

complete structure, for which the stiffness matrix is B_z. A natural frequency of this beam occurs when $|B_z|$ is zero. It may be shown [21] that this equation is satisfied only when

$$sin(\alpha_z) = 0 \tag{52}$$

which requires that

$$\alpha_z = i\pi, \quad (i = 1, 2, 3, ...).$$

Hence, the number of natural frequencies of the simply supported beam exceeded by ω^* is j_{cz} where

$$j_{cz} \quad \text{is the highest integer} \leq \frac{\alpha_z}{\pi}.$$

Then,

$$j_{fz} = j_{cz} - sB_z,$$

where j_{fz} is the component of j_m corresponding to the in-plane flexural modes. Similarly, j_{fy} can be calculated from

$$sin(\alpha_y) = 0 \tag{53}$$

which requires that

$$\alpha_y = i\pi, \quad (i = 1, 2, 3, ...).$$

Hence,

$$j_{cy} \quad \text{is the highest integer} \leq \frac{\alpha_y}{\pi}.$$

where, B_y is the stiffness matrix for the simply supported beam, when its out-of-plane flexural vibration is considered.

Then,

$$j_0 = \sum_{k=1}^{NE} j_m, \tag{54}$$

where

$$j_m = j_a + j_{fz} + j_{fy} + j_t.$$

Thus, exploiting this methodology, it is possible to converge on any required natural frequency. The mode corresponding to a complex eigenvector x_j can be taken as the real part of $X_j = x_j e^{i\omega_j t}$. (Based on the paper published by Wittrick and Williams [8], alternatively one could choose to take the imaginary part but the mode so calculated will be exactly the same as that obtaining from the real part but the origin of time shifted by a quarter period). To find the modes, one can then solve

the equation $K^{\Delta}_{DS}(\omega^{'})x = p_r$, where $\omega^{'}$ represents either the upper or lower bound on ω_j at the stage when convergence, with the bisection process, is stopped and p_r is a *random* complex vector [8].

RESULTS AND NUMERICAL CHECKS

Numerical checks were performed to confirm the accuracy of the theory. First, the natural frequencies of (in and out-of-plane) transverse vibrations for non-rotating beams were studied. For simple uniform beams, the DFE leads to the 'exact' results, even when a single element mesh is considered (see for example, [6, 22, 23]).

Natural Frequencies of A Vertical Uniform Spinning Beam

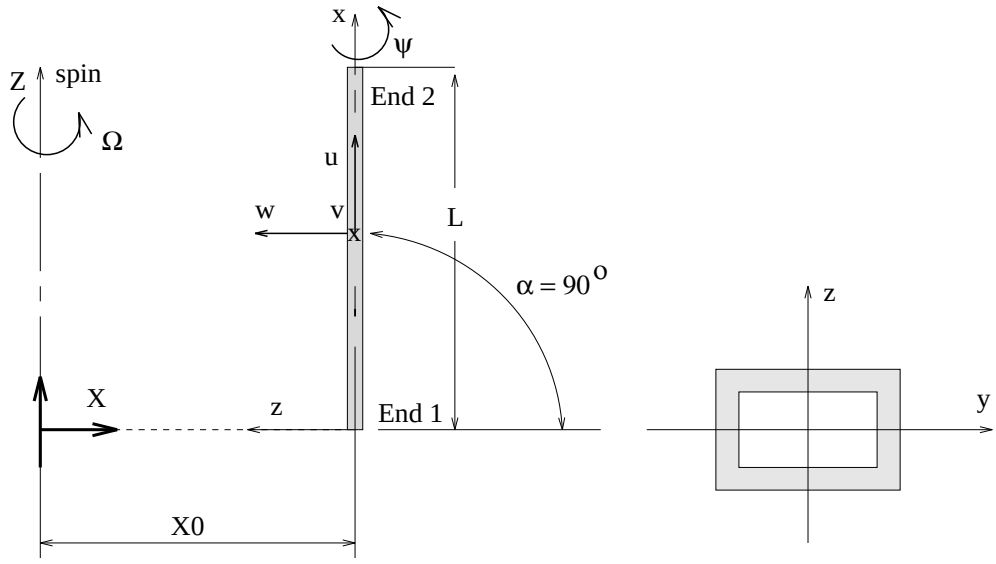

FIGURE 4: Rotating uniform beam geometry.

As an illustration of the possible application of the DFE developed here, a vertical cantilever rotating uniform beam ($\alpha = 90^o$) was studied. This example was originally given by Argyris and Mlejnek [4, 24]. The beam was considered to be attached to a rigid hub which is spinning about the z axis (see Figure 4 for details).

The following cross-sectional properties were used in the calculation:
(i) moments of inertia (Iyy) = 1.66493 m^4 and (Izz) = 2.49739 m^4, respectively,
(ii) Young's modulus (E) = 1.03422E+11 N/m^2,
(iii) cross-section area (A) = 1.032256 m^2,
(iv) density (ρ) = 230.6593 kg/m^3.
The length of the beam was assumed to be 1.016 m and $X_0 = 2L = 2.032$ m.

For simplicity it was assumed, that the shear centre and centroid of the cross section of the beam coincide. Furthermore, in this case, there is no coupling between the axial displacements and those due to the out-of-plane (flapping) or in-plane (lead-lag) vibrations ($\cos\alpha = 0.$). Hence, the axial displacement, in this case, can be treated separately.

From Eqs. (26-28 and 49) we conclude that the preload has no influence on the beam modal frequencies for this particular configuration and the centripetal acceleration term tends to soften the system in both directions. These conclusions are supported by the results illustrated in Figures 5 and 6. It can be seen that the lead-lag frequency (in the $x-y$ plane) increases and that in the $x-z$ plane (flapping frequency) decreases with increasing rotational speed. As presented by Laurenson [4] the spreading of this system frequencies is a normal characteristic when the Coriolis acceleration terms are included. For the particular beam orientation shown in Figure 4 we see that the first-mode frequency in the $x-z$ plane goes to zero as the spin rate approaches the non-spin frequency ω_{z0}. This zero structural frequency condition corresponds to the situation of an unstable system [4].

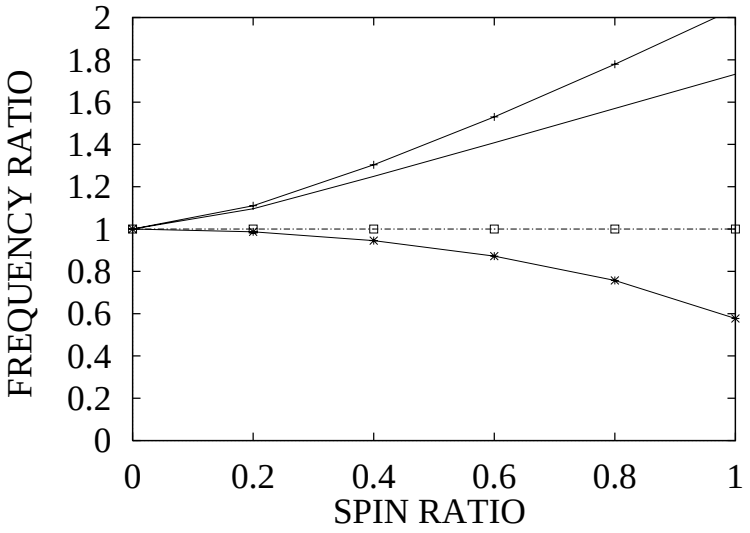

FIGURE 5: Comparison of spin-induced effects for $\alpha = 90^o$; the FREQUENCY RATIO- (first lead-lag mode $(\omega_x)/\omega_{x0}$ vs SPIN RATIO- Ω/ω_{z0}; ——, preload plus centripetal and Coriolis Accelerations included; —∗—, only the centripetal Acceleration included; —+—, only the Coriolis Acceleration included ; —□—, only the preload included.

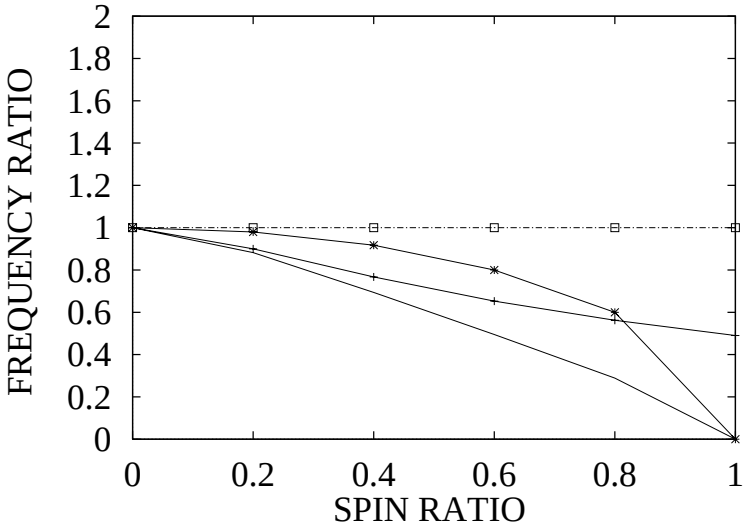

FIGURE 6: Comparison of spin-induced effects for $\alpha = 90^o$; the FREQUENCY RATIO- (first flapping mode $(\omega_z)/\omega_{z0}$ vs SPIN RATIO- Ω/ω_{z0}; ——, preload plus centripetal and Coriolis Accelerations included; —∗—, only the centripetal Acceleration included; —+—, only the Coriolis Acceleration included ; —□—, only the preload included.

Dynamic Characteristics of A Uniform Rotating Radial Beam

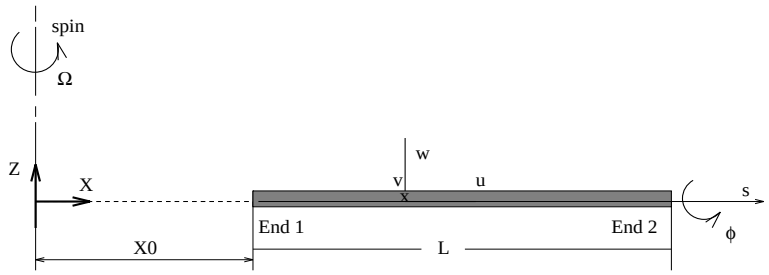

FIGURE 7: A cantilever uniform radial beam.

A cantilever uniform radial beam ($\alpha = 0.$) was studied. The beam was considered to be attached to a rigid hub which is spinning about the z axis with constant velocity Ω (Figure 7). For simplicity it was again assumed, that the shear centre and the centroid of the cross section of the beam coincide. Furthermore, because of the geometry of the radial beam, the out-of-plane (flapping) flexural vibration is uncoupled from axial and in-plane (lead-lag) flexural vibrations ($\sin\alpha = 0.$). Hence, the torsional and (flapping) flexural vibrations can be studied separately and they were not considered in the following example.

The following cross-sectional properties were used in the calculation:
(i) bending rigidity ($H_{fz} = EI_{zz}$) = $2.E + 6$ N.m^2,
(ii) mass per unit length (m) = 12. kg/m,
(iii) tensional rigidity (EA) = 2.4E+9 N.
(iv) spinning velocity (Ω) $\approx$4900 rad/sec.
The length of the beam was assumed to be 1.0 m. The results corresponding to this study are presented in Table 1. An eigenvalue analysis at zero rotational speed (which could certainly be carried out by hand), serves as a basis for comparison. These results were obtained exploiting the DFE method which, in this case, gives exact results when even only one element is used. Subsequently, the rotational velocity is increased to (Ω) $\approx$4900 rad/sec and, on the assumption that only centrifugal forces are acting upon the structure, a further eigenvalue analysis is carried out. Hence, we have a summary view of the qualitative and quantitative effects of the centrifugal forces on the eigenvalue spectrum. As a typical effect, we note a spreading of the frequency spectrum: the first, the second and the fourth (flexural) frequencies rise distinctly and the second (which is an extensional one) falls. The eigenmodes found in these cases are real and they represent the uncoupled extensional

and bending displacements. If the Coriolis forces are now introduced, as is more realistic, we note their influence on the frequency spectrum: on the first bending mode, the Coriolis forces have an important effect, since the eigenfrequency falls about 9%. The second and fourth eigenfrequencies fall, but the difference is not as important as for the first one (about 1.5% and 0.5%, respectively). The third eigenfrequency of the rotating structure involves axial displacement, now combined with in-plane bending (lead-lag). The increase in frequency amounts to about 10%. We can thus conclude that the Coriolis forces possess a considerable influence on this type of structures and should be taken into consideration for similar systems like complete turbine and compressor blades and spin-stabilized space structures. Other types of Coriolis forces, like those arising from combined in-plane bending and out-of-plane bending, have also a considerable effect on similar structures and should be certainly taken into account [4]. Another type of Coriolis force encountered in the case of spinning turbine rotor and rotating shafts arises from bending-bending-torsion displacements and has even larger impacts on the eigenfrequencies of these types of structures as reported by Argyris and Mlejnek [24]. The DFE method can be also extended to cover more complex cases.

CONCLUSION

A DFE method to calculate the natural frequencies and mode shapes of vibration of uniform spinning beams and rotating structures made of beams is presented. The expressions for the frequency dependent trigonometric shape functions of uncoupled, bending and axial, vibrations are used to find the DFE stiffness matrix, which, in this case, is Hermitian. This enables the Wittrick-Williams algorithm [8, 10] to be used to find the natural frequencies of rotating beam-made structures. Numerical results, on natural frequencies, are in agreement with published results and showed that the Coriolis forces have a considerable influence on rotating structures and should be taken into consideration.

ACKNOWLEDGMENTS

Special thanks to professor G. Dhatt, from l'INSA de Rouen (France), for valuable comments and scientific discussions. The authors are grateful to the Ministry of Culture and Higher Education of Iran for awarding a scholarship to the first author which made this work possible. The authors wish also to acknowledge the assistance of the Natural Sciences and Engineering Research Council of Canada which also supported this work.

TABLE 1: Natural frequencies of rotating bending-tension coupled radial beam ($\alpha = 0$) with cantilever end conditions.

	Frequency (μ_i†)			
i	λ‡ = 0	$\lambda = 12$	$\lambda = 12$	$\lambda = 12$
	No Forces Included	Centrifugal Forces Only	Centrifugal + Centripetal Forces	Centrifugal + Centripetal + Coriolis Forces
1	3.52	13.17	5.43	4.96
2	22.03	37.60	35.64	35.12
3	54.41	54.41	53.07	58.37
4	61.70	79.62	78.71	78.31

† Non-dimensionalized form of Ω ; $\lambda = \left(\frac{m\Omega^2 L^4}{H_{fz}}\right)^{1/2}$.

‡ Non-dimensionalized form of ω_i ; $\mu_i = \left(\frac{m\omega^2 L^4}{H_{fz}}\right)^{1/2}$.

References

[1] Likins, P. W., Barbera, F. J. and Baddeley Victor, 1973, "Mathematical Modeling of Spinning Elastic Bodys for Modal Analysis", AIAA Journal Vol. 11, pp. 1251-1258.

[2] Simpson, A., 1973, "Calculation of natural frequencies and modes of steadily rotating systems: a teaching note", The Aeronautical Quarterly Vol. 24, pp. 139-146.

[3] Meirovitch, L., 1974, "A new method of solution of the eigenvalue problem for gyroscopic systems", AIAA Journal Vol. 12, pp. 1337-1342.

[4] Laurenson, R. M., 1976, "Modal Analysis of Rotating Flexible Structures", AIAA Journal Vol. 14(10), pp. 1444-1450.

[5] Hoa, S. V., 1979, "Vibration of A Rotating Beam With Tip Mass", Journal of Sound and Vibration, Vol. 67(3), pp. 369-381.

[6] Hodges, D. H. and Rutkowski, M. J., 1981, "Free-Vibration Analysis of Rotating Beams by a Variable-Order Finite-Element Method", AIAA Journal, Vol. 19(11), pp. 1459-1466.

[7] Hashemi, S. M., Richard M. J. and Dhatt, G., 1997-A, A Dynamic Finite Element (DFE) Formulation for Free Vibration Analysis of Centrifugally Stiffened Uniform Beams, Proceeding of "16th CANadian Congress of Applied Mechanics (CANCAM 1997), June 1-6, Québec, Québec, pp. 443-444.

[8] W. H. Wittrick and Williams, F. W., 1982, "On the free vibration analysis of spinning structures by using discrete or distributed mass models", Journal of Sound and Vibration, Vol. 82(1), pp. 1–15.

[9] Hashemi, S. M., Richard M. J. and Dhatt, G., 1997-B, A Bernoulli-Euler Stiffness Matrix Approach for Vibrational Analysis of Spinning Linearly Tapered Beams, 42nd ASME Gas Turbine and Aeroengine Congress, June 2-5, Orlando, Florida.
Paper No. 97-GT-500.

[10] Williams, F. W. and Wittrick, W. H., 1970, "An automatic computational procedure for calculating natural frequencies of skeletal structures", International Journal of Mechanical Sciences, Vol. 12, pp. 12781–791.

[11] Wittrick, W. H. and Williams, F. W., 1971, "A general algorithm for computing natural frequencies of elastic structures", Quarterly Journal of Mechanics and Applied Mathematics, Vol. 24, pp. 263–284.

[12] Åkesson, B. Å, 1976 "Pfvibat- a computer program for plane frame vibration analysis by an exact method", International Journal for Numerical Methods in Engineering, Vol. 10, pp. 1221–1231.

[13] Banerjee, J. R., 1989, "Coupled bending-torsional dynamic stiffness matrix for beam elements", International journal for numerical methods in engineering, Vol.28, pp. 1283–1298.

[14] Hashemi, S. M., Richard, M. J. and Dhatt, G., 1996, "A Bernoulli-Euler Stiffness Matrix Approach for Vibrational Analysis of Linearly Tapered Beams", Proceeding of "Acoustics Week in Canada 1996", October 7-11, Calgary, Alberta, p. 87.

[15] Hashemi, S. M., Richard M. J. and Dhatt, G., 1999, "A New Dynamic Finite Element (DFE) Formulation For Lateral Free Vibrations of Euler-Bernoulli Spinning Beams Using Trigonometric Shape Functions", Journal of Sound and Vibration, Vol. 220(4), pp. 602–623.

[16] Hashemi, S. M., Richard M. J. and Dhatt, G., 1998, "A Dynamic Finite Element (DFE) Approach for Coupled Bending-Torsional Vibrations of Beams", The proceeding of the 39th AIAA/ASME/ASCE /AHS/ASC Structures, Structural Dynamics, and Materials Conference, Long Beach, CA, pp. 2614-2624. Paper No. 98-AIAA-2020.

[17] Hashemi, S. M. and Richard, M. J., 1998, "On The Coupled Bending-Torsional Natural Frequencies and Modes of Beams; A Frequency Dependent Dynamic Finite Element (DFE)", The proceeding of the Biennial Conference of the Canadian Society for Mechanical Engineering (CSME FORUM 1998), pp. 468–475.

[18] Bellezza, F., Lanari, L., and Ulivi, G., 1990, "Exact modelling of the flexible slewing link" Proceeding of the 1990 IEEE International Conference on Robotics and Automation, MAy 13–18, Cincinati, OH, pp. 734–739.

[19] Dhatt, G. and Touzot, G., 1981, "Une présentation de la méthode des éléments finis", Maloine S.A. Éditeur, Paris et Les presses de L'Université Laval, Québec, pp. 100-103, in French.

[20] Bathe, K. J., 1982, " Finite Element Procedures in Engineering Analysis" Englewood-Cliffs, N. J.: Prentice-Hall.

[21] Howson, W. P. and Williams F. W., 1973, "Natural frequencies of frames axially loaded Timoshenko members", Journal of sound and vibration, Vol. 26(4), pp. 503–515.

[22] Hashemi, S. M., 1998, "Free Vibrational Analysis of Rotating Beam-like Structures: A Dynamic Finite Element Approach", Ph.D. Thesis, Department of Mechanical Engineering, Laval University, Québec, Canada.

[23] Hashemi, S. M., Richard M. J., 1999, On the Natural Frequencies of Rotating Blades with Discontinuous Geometry: A Dynamic Finite Element (DFE) Formulation, Proceeding of "17th CANadian Congress of Applied Mechanics (CANCAM 1999), May 30 - June 3, Hamilton, Ontario, pp. 293-294.

[24] Argyris, J. and Mlejnek, H. P., 1991, "Texts on Computational Mechanics Volume V: Dynamic of Structures", Amesterdam: North-Holland.

Appendix A: Derivation of the governing equations

In the *undeformed* state the member lies in the $x-z$ plane, inclined at an arbitrary angle α with respect to the x direction and the coordinates (x_0, y_0, z_0) of the centroid of a general cross section are then given by (see Figure 2)

$$x_0 = X_0 + s\ \cos\alpha, \qquad y_0 = y_0, \qquad z_0 = s\ \sin\alpha. \tag{55}$$

where s is the distance measured along the member and X_0 is the radius at $s = 0$. Let the small deformation of the member be defined by the centroidal displacements $u(s,t), v(s,t)$ and $w(s,t)$, together with a torsional rotation $\psi(s,t)$, as shown in in Figure (2). Then the coordinates of the centroid of the deformed member are

$$x = x_0 + u\ \cos\alpha - w\ \sin\alpha, \qquad y = y_0 + v,$$

$$z = z_0 + u\ \sin\alpha + w\ \cos\alpha. \tag{56}$$

The position vector to the centroid of a general differential segment of the deformed member is given by

$$\vec{r} = x\ \vec{i} + y\ \vec{j} + z\ \vec{k} \tag{57}$$

The absolute angular velocity of the rotating system is assumed to be constant and is given by $\omega = \Omega\vec{k}$. Differentiating equation (57) twice with respect to time gives the acceleration vector as

$$\begin{aligned}\ddot{\vec{r}} = \Big\{&\ddot{u}\ \cos\alpha - \ddot{w}\ \sin\alpha - 2\ \dot{v}\ \Omega - x_0\Omega^2\ - \\ &u\ \Omega^2\ \cos\alpha + w\ \Omega^2\ \sin\alpha\Big\}\vec{i}\ + \\ \Big\{&\ddot{v} + 2\ \dot{u}\ \Omega\ \cos\alpha - 2\ \dot{w}\ \Omega\ \sin\alpha - v\ \Omega^2\Big\}\vec{j}\ + \\ &\{\ddot{u}\ \sin\alpha + \ddot{w}\ \cos\alpha\}\vec{k}\end{aligned} \tag{58}$$

Then, the components of acceleration in the local (elementary) coordinates are found as:

$$a_u = (\ddot{u} - u\ \Omega^2\ \cos^2\alpha) - 2\ \dot{v}\ \Omega\ \cos\alpha + (w\ \sin\alpha - x_0)\ \Omega^2\cos\alpha \tag{59}$$

$$a_v = 2\ \dot{u}\ \Omega\ \cos\alpha + (\ddot{v} - v\ \Omega^2) - 2\ \dot{w}\ \Omega\ \sin\alpha \tag{60}$$

$$a_w = (u + x_0)\ \Omega^2\cos\alpha\ \sin\alpha + 2\ \dot{v}\ \Omega\ \sin\alpha + (\ddot{w} - w\ \Omega^2\ \sin^2\alpha) \tag{61}$$

The final term in each of the equations for a_u and a_w is independent of time and represents the component of the steady state radial acceleration $x_0\Omega^2$. These terms give rise to a steady state deformation of the spinning structure. However, we consider small vibrations about the steady *deformed* state so that the last term in each of the equations for a_u and a_w can be ignored [8]. Since the components of acceleration of the centroid of a cross section are known, it is now a simple matter to write the equations of motion for an element of the beam.

Appendix B: Dynamic (Frequency Dependent) Extensional, Flexural and Torsional Shape Functions

The dynamic in-plane (lead-lag) flexural shape functions, mentioned earlier, are found to be as follows [22] (to find the expressions corresponding to the out-of-plane (flapping) displacements we have just to replace the subscript "z" by "y" in the following expressions):

$$N_1(\omega)_{fz} = \frac{(\alpha_z\beta_z)}{D_{fz}} * \{-\cos(\alpha_z\xi) + \cos(\alpha_z(1-\xi)) * \cosh(\beta_z) + \cos(\alpha_z) * \cosh(\beta_z(1-\xi)) - \cosh(\beta_z\xi) - \frac{\beta_z}{\alpha_z} * \sin(\alpha_z(1-\xi)) * \sinh(\beta_z) + \frac{\alpha_z}{\beta_z} * \sin(\alpha_z) * \sinh(\beta_z(1-\xi))\} \qquad (B1-a)$$

$$N_2(\omega)_{fz} = \frac{1}{D_{fz}} * \{\beta_z * [\cosh(\beta_z(1-\xi)) * \sin(\alpha_z) - \cosh(\beta_z) * \sin(\alpha_z(1-\xi)) - \sin(\alpha_z\xi)] + \alpha_z * [\cos(\alpha_z(1-\xi)) * \sinh(\beta_z) - \cos(\alpha_z) * \sinh(\beta_z(1-\xi)) - \sinh(\beta_z\xi)]\} \qquad (B1-b)$$

$$N_3(\omega)_{fz} = \frac{(\alpha_z\beta_z)}{D_{fz}} * \{-\cos(\alpha_z(1-\xi)) + \cos(\alpha_z\xi) * \cosh(\beta_z) - \cosh(\beta_z(1-\xi)) + \cos(\alpha_z) * \cosh(\beta_z\xi) - \frac{\beta_z}{\alpha_z} * \sin(\alpha_z\xi) * \sinh(\beta_z) + \frac{\alpha_z}{\beta_z} * \sin(\alpha_z) * \sinh(\beta_z\xi)\} \qquad (B1-c)$$

$$N_4(\omega)_{fz} = \frac{1}{D_{fz}} * \{\beta_z * [-\cosh(\beta_z\xi) * \sin(\alpha_z) + \sin(\alpha_z(1-\xi)) + \cosh(\beta_z) * \sin(\alpha_z\xi)] - \alpha_z * [\cos(\alpha_z\xi) * \sinh(\beta_z) + \sinh(\beta_z(1-\xi)) + \cos(\alpha_z) * \sinh(\beta_z\xi)]\} \qquad (B1-d)$$

The extensional dynamic shape functions are found to be as

$$N_1(\omega)_a = \cos(\eta\xi) - \cos(\eta) * \frac{\sin(\eta\xi)}{D_a} \qquad (B1-e/g)$$

$$N_2(\omega)_a = \frac{\sin(\eta\xi)}{D_a} \qquad (B1-f/h)$$

and torsional dynamic shape functions are simply found by changing a to t and replacing η by τ in these expressions, and

$$D_{fz} = (\alpha_z\beta_z) * \{-2 * (1 - \cos(\alpha_z) * \cosh(\beta_z)) + (\frac{\alpha_z^2 - \beta_z^2}{\alpha_z\beta_z}) * \sin(\alpha_z) * \sinh(\beta_z)\}\ , \qquad (B1-i)$$

$$D_a = \sin(\eta)\ , \quad D_t = \sin(\tau)\ . \qquad (B1-j,k)$$

The following figures represent the standard (static) cubic Hermite type basis functions, the dynamic besis functions for a non-rotating beam, the dynamic basis functions and dynamic shape functions for the flexural vibrations of a rotating beam.

FIGURE 8: The basis functions $(P_i)_{fz}, i = 1, 2, 3, 4)$ for in-plane (lead-lag) flexural vibration of a uniform beam rotating in horizontal plane; E=1 GPa, A=1 m^2, L=1 m, ρ =1 kg/m^3, and I=1 m^4. (a) standard (static) cubic baisis functions; (b) dynamic basis function for a non-rotating beam; (c) dynamic basis function for a rotating beam and $\lambda = \Omega.l^2.\sqrt{m/E.I}$ =12; — , P_1; –o–, P_2; –+–, P_3; –⋆-, P_4.

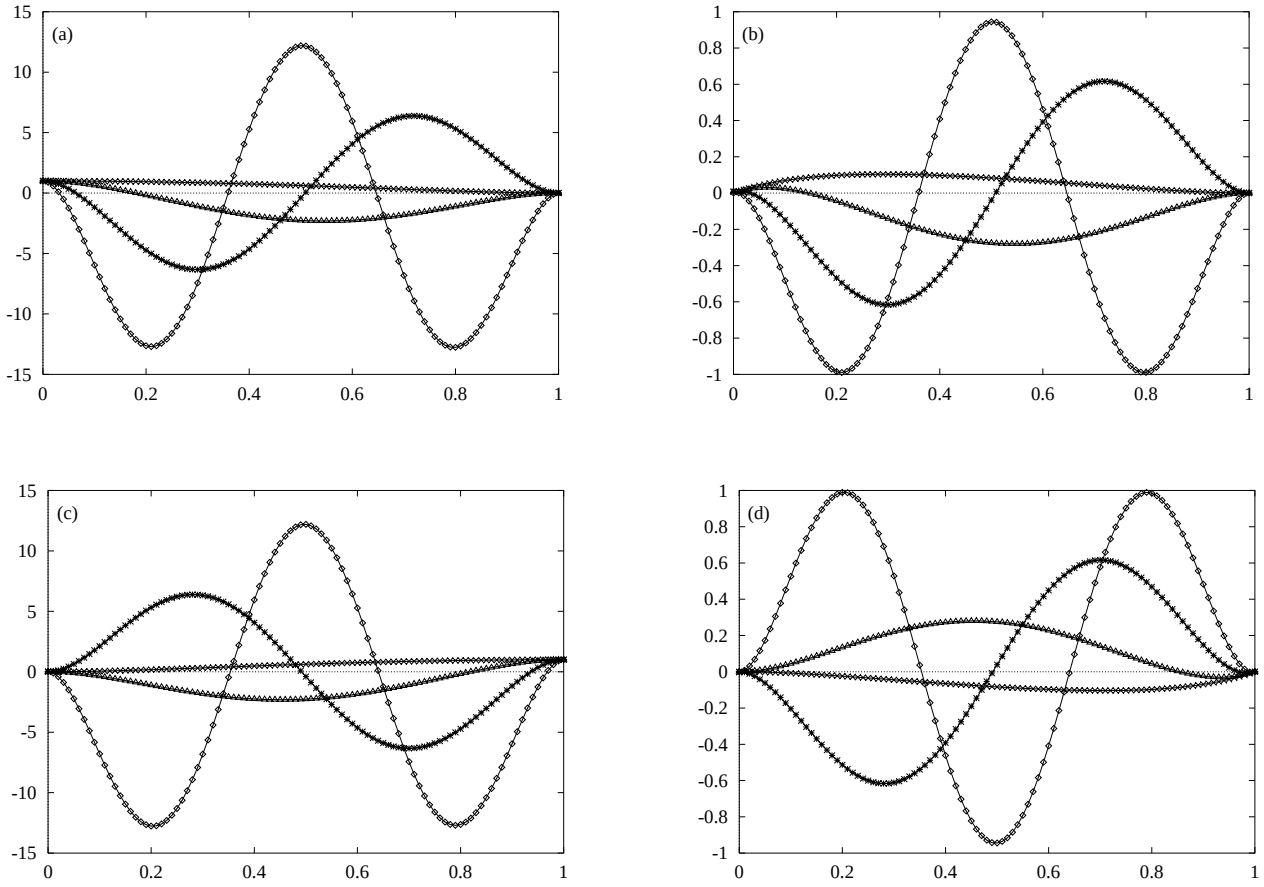

FIGURE 9: The variation of the dynamic in-plane (lead-lag) flexural shape functions N_i vs frequency changes for a uniform beam rotating in horizontal plane; E=1 GPa, A=1 m^2, L=1 m, ρ =1 kg/m^3, I=1 m^4, and $\lambda = \Omega.l^2.\sqrt{m/E.I}$ =12. (a) N_1; (b) N_2; (c) N_3; (d) N_4; $-_{\times}$, ω_1, 1st natural frequency; $-_{\triangle}$, ω_2, 2nd natural frequency; $-\star$, ω_3, 3rd natural frequency; $-\diamond$, ω_4, 4th natural frequency.

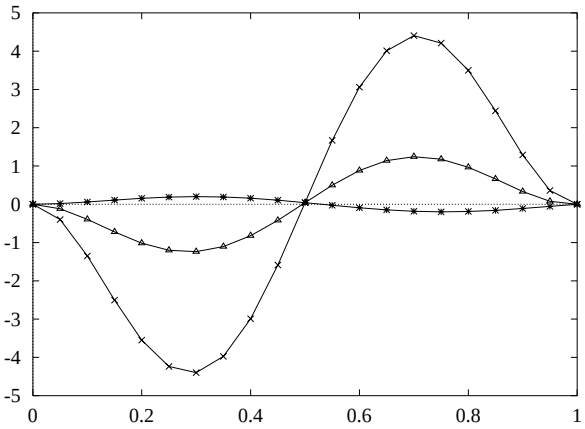

FIGURE 10: The change of the fourth dynamic shape function, N_4, at the third natural frequency, ω_3, vs spinning speed for the same beam as in Figures 9. $-_{\times}$, Ω=4 rad/s; $-_{\triangle}$, Ω=8 rad/s; $-\star$, Ω=12 rad/s.

Appendix C: The "DFE" Stiffness Matrices

$[K_{DS}]^k_{DEV} =$

$$\begin{bmatrix}
0 & 0 & 0 & 0 & 0 & 0 & 0 & 0 & 0 & 0 & 0 & 0 \\
 & (Kz)_{11} & (Kz)_{12} & 0 & 0 & 0 & 0 & (Kz)_{13} & (Kz)_{14} & 0 & 0 & 0 \\
 & & (Kz)_{22} & 0 & 0 & 0 & 0 & (Kz)_{23} & (Kz)_{24} & 0 & 0 & 0 \\
 & & & (Ky)_{11} & (Ky)_{12} & 0 & 0 & 0 & 0 & (Ky)_{13} & (Ky)_{14} & 0 \\
 & & & & (Ky)_{22} & 0 & 0 & 0 & 0 & (Ky)_{23} & (Ky)_{24} & 0 \\
 & & & & & 0 & 0 & 0 & 0 & 0 & 0 & 0 \\
 & & & & & & 0 & 0 & 0 & 0 & 0 & 0 \\
 & & & & & & & (Kz)_{33} & (Kz)_{34} & 0 & 0 & 0 \\
 & & Sym. & & & & & & (Kz)_{44} & 0 & 0 & 0 \\
 & & & & & & & & & (Ky)_{33} & (Ky)_{34} & 0 \\
 & & & & & & & & & & (Ky)_{44} & 0 \\
 & & & & & & & & & & & 0
\end{bmatrix}$$

where; $(Kz)_{ij} = \int_0^1 -\frac{1}{l_k}(T_{DEV}) * N_i^{'}(\omega)_{fz} * N_j^{'}(\omega)_{fz}.d\xi,$
and $\quad (Ky)_{ij} = \int_0^1 -\frac{1}{l_k}(T_{DEV}) * N_i^{'}(\omega)_{fy} * N_j^{'}(\omega)_{fy}.d\xi;\ (i,j = 1,2,3,4).$

$[K_{DS}]^k_{COR} =$

$$\begin{bmatrix}
 & -uv_{11} & -uv_{12} & & & 0 & & -uv_{13} & -uv_{14} & & & 0 \\
uv_{11} & & & -vw_{11} & -vw_{12} & 0 & uv_{21} & & & -vw_{13} & -vw_{14} & 0 \\
uv_{12} & & & -vw_{21} & -vw_{22} & 0 & uv_{22} & & & -vw_{23} & -vw_{24} & 0 \\
 & vw_{11} & vw_{21} & & & 0 & & vw_{31} & vw_{41} & & & 0 \\
 & vw_{12} & vw_{22} & & & 0 & & vw_{32} & vw_{42} & & & 0 \\
0 & 0 & 0 & 0 & 0 & 0 & 0 & 0 & 0 & 0 & 0 & 0 \\
 & -uv_{21} & -uv_{22} & & & 0 & & -uv_{23} & -uv_{24} & & & 0 \\
uv_{13} & & & -vw_{31} & -vw_{32} & 0 & uv_{23} & & & -vw_{33} & -vw_{34} & 0 \\
uv_{14} & & & -vw_{41} & -vw_{42} & 0 & uv_{24} & & & -vw_{43} & -vw_{44} & 0 \\
 & vw_{13} & vw_{23} & & & 0 & & vw_{33} & vw_{43} & & & 0 \\
 & vw_{14} & vw_{24} & & & 0 & & vw_{34} & vw_{43} & & & 0 \\
0 & 0 & 0 & 0 & 0 & 0 & 0 & 0 & 0 & 0 & 0 & 0
\end{bmatrix}$$

where; $uv_{ij} = (2ml_k i\omega\Omega\cos\alpha)\int_0^1 N_i(\omega)_a * N_j(\omega)_{fz}.d\xi;\ (i = 1,2\ ;\ j = 1,2,3,4),$
and $\quad vw_{jk} = (2ml_k i\omega\Omega\sin\alpha)\int_0^1 N_i(\omega)_{fz} * N_j(\omega)_{fy}.d\xi;\ (j,k = 1,2,3,4).$

$$[K_{DS}]^{k}_{CENT} =$$

$$\begin{bmatrix}
0 & 0 & 0 & (uw)_{11} & (uw)_{12} & 0 & 0 & 0 & 0 & (uw)_{13} & (uw)_{14} & 0 \\
 & 0 & 0 & 0 & 0 & 0 & 0 & 0 & 0 & 0 & 0 & 0 \\
 & & 0 & 0 & 0 & 0 & 0 & 0 & 0 & 0 & 0 & 0 \\
 & & & 0 & 0 & 0 & (uw)_{21} & 0 & 0 & 0 & 0 & 0 \\
 & & & & 0 & 0 & (uw)_{22} & 0 & 0 & 0 & 0 & 0 \\
 & & & & & 0 & 0 & 0 & 0 & 0 & 0 & 0 \\
 & & & & & & 0 & 0 & 0 & (uw)_{23} & (uw)_{24} & 0 \\
 & & & & & & & 0 & 0 & 0 & 0 & 0 \\
 & & & & & & & & 0 & 0 & 0 & 0 \\
 & & Sym & & & & & & & 0 & 0 & 0 \\
 & & & & & & & & & & 0 & 0 \\
 & & & & & & & & & & & 0
\end{bmatrix}$$

where; $(uw)_{ij} = (ml_k\ \Omega^2\ \cos\alpha.\sin\alpha)\ \int_0^1 N_i(\omega)_a * N_j(\omega)_{fy}.d\xi;\ \begin{cases} i = 1,2\ , \\ j = 1,2,3,4\ . \end{cases}$